Acta Crystallographica Section D
**Biological Crystallography**
ISSN 0907-4449

# Crystallization of soluble urokinase receptor (suPAR) in complex with urokinase amino-terminal fragment (1–143)

**Mingdong Huang,[a,b]* Andrew P. Mazar,[c] Graham Parry,[c] Abd Al-Roof Higazi,[d,e] Alice Kuo[d] and Douglas B. Cines[d]**

[a]State Key Laboratory of Structural Chemistry, Fujian Institute of Research on the Structure of Matter, Chinese Academy of Sciences, Fuzhou 350002, People's Republic of China, [b]Beth Israel Deaconess Medical Center, Boston, MA 02460, USA, [c]Attenuon, LLC, 10130 Sorrento Valley Road, Suite B, San Diego, CA 92121, USA, [d]Department of Pathology and Laboratory Medicine, University of Pennsylvania Medical Center, 513A Stellar-Chance, 422 Curie Boulevard, Philadelphia, PA 19104, USA, and [e]Department of Clinical Biochemistry, Hadassah Medical Center, Jerusalem, Israel

Correspondence e-mail: mhuang@fjirsm.ac.cn

Received 20 July 2004
Accepted 3 May 2005



Urokinase-type plasminogen activator (urokinase, uPA) and its receptor, uPAR, have been implicated in cell adhesion, migration, tissue remodelling and tumour-cell invasion. uPAR has three domains and is anchored to membranes by a glycosyl-phosphatidylinositol (GPI) anchor. Recombinant uPAR without its GPI anchor, soluble uPAR (suPAR), tends to oligomerize, making it difficult to crystallize. The amino-terminal fragment (ATF) of uPA is the major receptor-binding determinant in suPAR and binds to suPAR with nanomolar affinity, indistinguishable from membrane-bound uPAR. It is shown that uPA is capable of dissociating the oligomerization of suPAR and the crystallization of the suPAR–ATF complex is reported here. The resulting crystals diffract to 3.1 Å using a synchrotron X-ray source.

## 1. Introduction

Urokinase-type plasminogen activator (uPA) and its cellular receptor (uPAR) have received extensive study as one of the two primary endogenous systems that mediate plasminogen activation. More recently, a broader role for uPA/uPAR in cell adhesion, migration, tissue remodelling and signal transduction has been suggested (Chapman, 1997; Preissner *et al.*, 1999; Andreasen *et al.*, 2000). These proposed functions of uPA/uPAR have led to intense interest in understanding its contribution to physiologic (wound repair, angiogenesis) and diverse pathophysiologic (*e.g.* inflammation, tumour metastasis) processes involving cell migration.

The capability of uPAR to interact with an array of extracellular molecules is the basis of its biological functions. uPAR (CD87) (Sitrin *et al.*, 1994; Vassalli *et al.*, 1985; Stoppelli *et al.*, 1985) is a heterogeneously glycosylated single-chain membrane-associated protein that can be expressed on the surface of leukocytes, endothelial and vascular smooth muscle cells, fibroblasts, trophoblasts and various types of tumour cells (Vassalli *et al.*, 1991). uPAR is anchored to the plasma membrane of cells by a glycosylphosphatidylinositol (GPI) moiety that is added concurrently with the post-translational removal of the COOH-terminal signal sequence at Gly283 (Ploug *et al.*, 1991; Moller *et al.*, 1992). uPAR localizes and promotes the proteolytic activities of uPA on the surface of cells (Ellis *et al.*, 1989; Stephens *et al.*, 1989; Duval-Jobe & Parmely, 1994). In addition to converting plasminogen to plasmin, uPA is capable of cleaving fibronectin, hepatocyte growth factor and other substrates that may be implicated in cell adhesion and migration. Plasmin generated by uPA itself has broad proteolytic specificity and is capable of directly degrading several extracellular matrix proteins and activating the matrix metalloproteases (MMPs) type IV collegenase and stromolysin-1 from their zymogen forms (pro-MMPs). At a subnanomolar affinity, uPAR binds to the somatostatin B domain of vitronectin (Wei *et al.*, 1994), an adhesive matrix protein that contains the Arg-Gly-Asp (RGD) adhesion domain and serves as a ligand for several integrin receptors. uPAR itself is also capable of binding directly to $\beta1$, $\beta2$ and $\beta3$ containing integrin heterodimers (Magdolen *et al.*, 1996; Butcher & Picker, 1996; Chavakis *et al.*, 2001; Tarui *et al.*, 2001).

uPAR binds uPA with a $K_d$ of 0.28 n*M* (Ploug *et al.*, 1998) to form a stable complex with a slow off-rate (Roldan *et al.*, 1990; Cubellis *et al.*, 1986; Barnathan *et al.*, 1990). The amino-terminal fragment (ATF) of uPA (amino acids 1–143) binds to uPAR with an affinity ($K_d$ of

0.28 n*M*; Ploug *et al.*, 1998) comparable to full-length uPA. Alanine-scanning mutagenesis has identified residues Asn22, Asn27, His29 and Trp30 in the Ω loop of the growth-factor domain of uPA as being required for the binding to uPAR (Hoyer-Hansen *et al.*, 1992; Magdolen *et al.*, 1996; Ploug *et al.*, 1998; Quax *et al.*, 1998).

It has been hypothesized that the mature uPAR folds into three domains, each containing 81–87 residues (Ploug & Ellis, 1994). The structure of uPAR and the arrangement of the three domains are unknown. Soluble uPAR variants (suPAR), consisting of residues 1–277 without the GPI anchor, have been identified under physiological conditions and in higher concentrations in pathological conditions such as in patients with malignancy (Pappot *et al.*, 1997; Chavakis *et al.*, 2001) or paroxysmal nocturnal haemoglobinuria (Ronne *et al.*, 1995; Gao *et al.*, 2002). suPAR binds exogenous uPA with a $K_d$ in the subnanomolar range, indistinguishable from the natural GPI-anchored full-length uPAR (Ploug & Ellis, 1994), which indicates that suPAR is an appropriate candidate for the study of uPA–uPAR interactions *in vitro*.

uPAR was observed to dimerize in detergent-resistant lipid rafts on cell surface (Cunningham *et al.*, 2003). Recombinant suPAR also tends to form an oligomer in aqueous solution at the concentrations required for protein crystallization, posing great difficulties in studying its crystal structure. Our studies indicate that the addition of urokinase largely dissociates the suPAR oligomer, leading to the formation of uPA–suPAR complexes in a 1:1 ratio (Shliom *et al.*, 2000). Regulation of uPAR oligomerization by uPA was further observed *in vivo* at the cellular level (Sidenius *et al.*, 2002). Thus, ligand binding to suPAR appears to be a reasonable approach to obtaining homogeneous preparation of suPAR, potentially allowing the study of its crystal structure in a biologically relevant conformation. Here, we report the crystallization of the ATF–suPAR complex and the preliminary crystallographic characterization of the crystals.

## 2. Experimental

### 2.1. Expression of suPAR

cDNA encoding soluble human uPAR (amino acids 1–277) was generated by PCR using vector pGEM-uPAR (provided by F. Blasi, Milan) as the template. The fragments were digested with *Bgl*II and *Xho*I and directionally subcloned into the expression vector (pMT/BiP/V5, Invitrogen) to yield pMT/BiP/V5-suPAR. Recombinant wild-type suPAR was expressed using the *Drosophila* Schneider S2 cells (DES system, Invitrogen) according to the manufacturer's recommendations. For preparative expression, S2 cell-culture supernatants were filtered and the media loaded onto a DEAE-Sephadex column equilibrated with 10 m*M* phosphate buffer pH 7.0. The column was then eluted with a gradient of 0–0.5 *M* NaCl in 10 m*M* phosphate buffer pH 7.0 and the suPAR-containing fractions were identified by Western blotting. Fractions containing monomeric suPAR were pooled, concentrated and further purified using C8 RP-HPLC. Crude suPAR (20 mg total protein) was loaded in a volume of 2 ml onto a semi-preparative (10 × 25 cm) C8 column and eluted at a flow rate of 4 ml min$^{-1}$ with a linear gradient of 0–100% solvent *B*, where solvent *A* was 100% $H_2O$/0.1% trifluoroacetic acid (TFA) and solvent *B* was 100% acetonitrile/0.1%TFA. suPAR eluted as a single broad peak under these conditions with a retention time of approximately 24 min. SDS–PAGE analysis of suPAR demonstrated a single major peak at 43 kDa under reducing conditions. Yields were typically 15–20 mg per litre of S2 cell-culture supernatant.

### 2.2. Expression of urokinase amino-terminal fragment 1–143

Recombinant ATF was also expressed in the *Drosophila* S2 system as a secreted protein, similar to the preparation of suPAR. Preparative amounts of ATF were purified using SP-Sephadex in 50 m*M* bicine buffer pH 8.0 with a 0–0.5 *M* NaCl gradient. Fractions containing ATF, identified by Western blotting using a polyclonal antibody against urokinase (kindly provided by American Diagnostica), were concentrated using a Millipore YM-3 membrane and purified using C8 RP-HPLC. Crude ATF was loaded in a 2 ml volume onto a semi-preparative (10 × 25 cm) C8 column and eluted at a flow rate of 4 ml min$^{-1}$ with a linear gradient of 0–100% solvent *B*, where solvent *A* was 100% $H_2O$/0.1% TFA and solvent *B* was 100% acetonitrile/0.1%TFA. ATF eluted as a single broad peak under these conditions. Yields ranged from 10 to 20 mg protein per litre of S2 culture supernatant. The protein was characterized by SDS–PAGE under reducing and non-reducing conditions.

### 2.3. Preparation of complexes of suPAR with ATF and its crystallization

The complex was formed by incubating ATF with suPAR in a 2:1 molar ratio at room temperature in 50 m*M* HEPES and 100 m*M* NaCl pH 7.4 and was purified using a Superdex75 gel-filtration column and concentrated to about 5 mg ml$^{-1}$ for crystallization trials. Crystals of the complex were grown in a sitting-drop setup with a precipitant condition of either (i) 1.575 *M* ammonium sulfate, 0.1 *M* HEPES pH 7.5 (Fig. 1*a*) or (ii) 1.3 *M* sodium phosphate, 0.1 *M* HEPES pH 7.5 (Fig. 1*b*). In ammonium sulfate, crystals typically appeared from the crystallization drop in about a week, while in phosphate crystals took about a month to grow. For X-ray diffraction data collection, the crystal was briefly (<1 s) dipped into a mother-liquor solution containing 25% ethylene glycol and immediately frozen to 113 K in a liquid-nitrogen stream prior to data collection. X-ray diffraction data were collected either with synchrotron X-ray sources or with an in-house 5 kW Cu X-ray power source focused with an Osmic confocal mirror to 0.2 × 0.2 mm and were recorded on a MAR300 image plate.

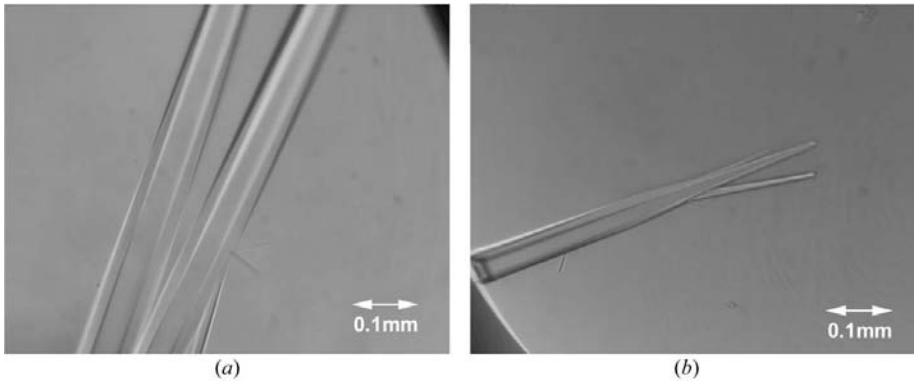


**Figure 1**
Crystals of suPAR–ATF complex from different crystallization conditions: (*a*) 1.575 *M* ammonium sulfate, (*b*) 1.3 *M* sodium phosphate.

## 3. Results and discussion

Urokinase receptor (uPAR) interacts not only with its ligand, urokinase, but also with

several other cellular proteins, including vitronectin, integrins (Wei *et al.*, 1996), LRP (Czekay *et al.*, 2001) and uPAR-associated protein (uPARAP; Sheikh *et al.*, 2000; Behrendt *et al.*, 2000), and has been implicated in several biological processes, such as cell adhesion, migration, tissue remodelling, arteriosclerosis and tumour-cell invasion. However, the crystal structure of uPAR and the structural basis of its interactions with uPA and extracellular molecules remain unknown. Here, we report the crystallization of soluble uPAR in complex with the amino-terminal fragment (ATF) of uPA, the uPAR-binding domain of uPA. The crystals can be formed at physiological pH either with ammonium sulfate or sodium phosphate as precipitants. The SDS–PAGE of the washed suPAR–ATF crystal (Fig. 2) is similar to that of the starting materials, indicating the existence of both suPAR and ATF inside the crystal.

The crystals diffracted to 3.5 Å at room temperature (297 K) with an in-house X-ray source. Freezing the crystal at low temperature (100 K) in order to increase its lifetime in the synchrotron X-ray beam turned out to be difficult: the crystals cracked or broke in the majority of common cryoprotectant solutions. After an extensive search, it was found the crystals can be flash-frozen without cracking if soaked into the mother liquor containing 25% ethylene glycol only very briefly (<1 s) and then placed immediately into the liquid-nitrogen stream. Such frozen crystals diffracted to a resolution comparable to room-temperature crystals. This protocol was used to collect synchrotron data. Data-collection statistics are given in Table 1.

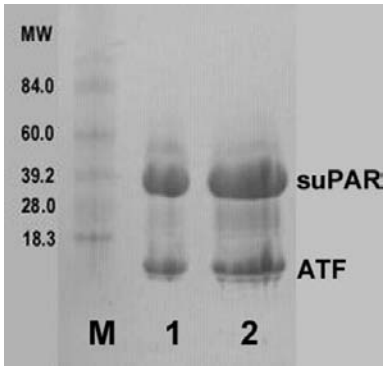


**Figure 2**
Reducing SDS–PAGE (8–25%) shows that the crystals contain both suPAR and ATF (lane 1) and are more homogeneous than the starting material (lane 2). Lane M contains protein molecular-weight standards.

**Table 1**
Data-collection statistics for suPAR–ATF crystal from the ammonium sulfate condition.

Values in parentheses are for the last resolution shell.

| | |
|---|---|
| Unit-cell parameters (Å, °) | $a$ = 131.9, $b$ = 131.9, $c$ = 106.5, $\alpha$ = 90, $\beta$ = 90, $\gamma$ = 120 |
| X-ray source | APS IMCA |
| Wavelength (Å) | 0.97923 |
| Temperature (K) | 100 |
| Resolution (Å) | 3.1 |
| Total no. of observations | 232215 |
| No. of unique reflections | 16170 (1226) |
| Overall redundancy | 14.4 |
| Completeness (%) | 83.6 (74.0) |
| $R_{\rm merge}$† | 0.131 (0.523) |
| $I/\sigma(I)$ | 6.7 (1.8) |

† $R_{\rm merge}(I) = \langle |I(i) - \langle I(h)\rangle| \rangle / \sum I(i)$, where $I(i)$ is the intensity of the $i$th observation and $\langle I\rangle$ is the mean intensity from multiple measurements of the $hkl$ reflection.

The crystals diffracted to 3.1 Å using a synchrotron X-ray source and belong to space group $P3_121$ or $P3_221$. The suPAR–ATF crystals contain two identical molecules in the asymmetric unit based on the Matthews coefficient (2.56 Å$^3$ Da$^{-1}$), showing a solvent content of 50.0% in the crystal. The two molecules are related by a twofold axis as shown by the self-rotation function (Fig. 3).

The crystallization of suPAR alone was unsuccessful in our hands, presumably owing to its tendency to form oligomers in aqueous solution at high concentration (5 mg ml$^{-1}$). We showed that single-chain urokinase (scuPA) is capable of dissociating suPAR oligomers and formed a well behaved suPAR–uPA complex (Shliom *et al.*, 2000). We have tried to crystallize both suPAR–scuPA and suPAR–ATF complexes. Only suPAR–ATF complex gave high-quality crystals as reported here.

We are currently solving the phase problem of the suPAR–ATF crystals by multiple approaches including molecular replacement and multiple anomalous dispersion of the SeMet derivative of the complex. The NMR structure of ATF has been published (Hansen *et al.*, 1994) and showed great inter-domain variability between kringle and growth-factor domains of ATF. However, we have been successful in positioning one of the NMR models into our suPAR–ATF crystal by the molecular-replacement method. No appropriate molecular-replacement model for suPAR can be found, so the structure of suPAR–ATF will be further approached by multiple anomalous dispersion of the selenomethionyl derivative of the complex. The structure of this complex will reveal the domain structure and domain organization of uPAR and the molecular details of interaction between uPAR and its ligand, providing a platform for rational design of small molecules to intervene in uPAR–uPA interactions.

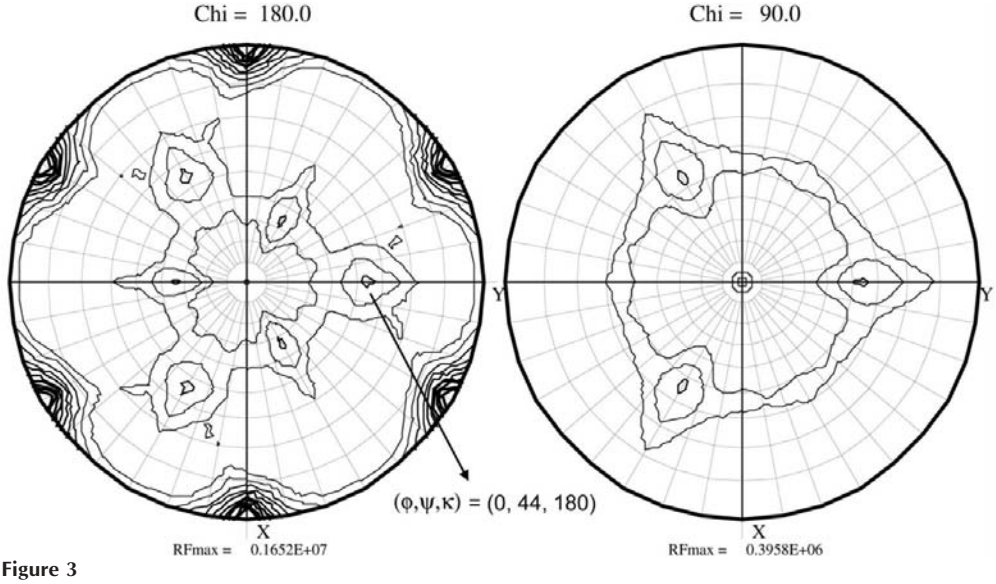


**Figure 3**
Self-rotation function of suPAR–ATF data set shows the position of the twofold axis (0, 44, 108°) that relates the suPAR–ATF dimer inside the asymmetric unit.

This work was supported by grants from the American Heart Association (0330089N), Chinese Academy of Sciences Hundred Talents Project (MH), NSFC-30430190 (MH), RO1-HL67381 (AH) and RO1-HL60169 (DC). We thank the APS IMCA beamline and BNL NSLS beamlines X8C and X12C for beam time to collect X-ray diffraction data.

## References

Andreasen, P. A., Egelund, R. & Petersen, H. H. (2000). *Cell. Mol. Life Sci.* **57**, 25–40.
Barnathan, E. S., Kuo, A., Rosenfeld, L., Kariko, K., Leski, M., Robbiati, F., Nolli, M. L., Henkin, J. & Cines, D. B. (1990). *J. Biol. Chem.* **265**, 2865–2872.
Behrendt, N., Jensen, O. N., Engelholm, L. H., Mortz, E., Mann, M. & Dano, K. (2000). *J. Biol. Chem.* **275**, 1993–2002.
Butcher, E. C. & Picker, L. J. (1996). *Science*, **272**, 60–66.
Chapman, H. A. (1997). *Curr. Opin. Cell. Biol.* **9**, 714–724.
Chavakis, T., Willuweit, A. K., Lupu, F., Preissner, K. T. & Kanse, S. M. (2001). *Thromb. Haemost.* **86**, 686–693.
Cubellis, M. V., Nolli, M. L., Cassani, G. & Blasi, F. (1986). *J. Biol. Chem.* **261**, 15819–15822.
Cunningham, O., Andolfo, A., Santovito, M. L., Iuzzolino, L., Blasi, F. & Sidenius, N. (2003). *EMBO J.* **22**, 5994–6003.
Czekay, R. P., Kuemmel, T. A., Orlando, R. A. & Farquhar, M. G. (2001). *Mol. Biol. Cell*, **12**, 1467–1479.
Duval-Jobe, C. & Parmely, M. J. (1994). *J. Biol. Chem.* **269**, 21353–21357.
Ellis, V., Scully, M. F. & Kakkar, V. V. (1989). *J. Biol. Chem.* **264**, 2185–2188.
Gao, W., Wang, Z., Bai, X., Li, Y. & Ruan, C. (2002). *Int. J. Hematol.* **75**, 434–439.
Hansen, A. P., Petros, A. M., Meadows, R. P., Nettesheim, D. G., Mazar, A. P., Olejniczak, E. T., Xu, R. X., Pederson, T. M., Henkin, J. & Fesik, S. W. (1994). *Biochemistry*, **33**, 4847–4864.
Hoyer-Hansen, G., Ronne, E., Solberg, H., Behrendt, N., Ploug, M., Lund, L. R., Ellis, V. & Dano, K. (1992). *J. Biol. Chem.* **267**, 18224–18229.
Magdolen, V., Rettenberger, P., Koppitz, M., Goretzki, L., Kessler, H., Weidle, U. H., Konig, B., Graeff, H., Schmitt, M. & Wilhelm, O. (1996). *Eur. J. Biochem.* **237**, 743–751.
Moller, L. B., Ploug, M. & Blasi, F. (1992). *Eur. J. Biochem.* **208**, 493–500.
Pappot, H., Hoyer-Hansen, G., Ronne, E., Hansen, H. H., Brunner, N., Dano, K. & Grondahl-Hansen, J. (1997). *Eur. J. Cancer*, **33**, 867–872.
Ploug, M. & Ellis, V. (1994). *FEBS Lett.* **349**, 163–168.
Ploug, M., Ostergaard, S., Hansen, L. B., Holm, A. & Dano, K. (1998). *Biochemistry*, **37**, 3612–3622.
Ploug, M., Ronne, E., Behrendt, N., Jensen, A. L., Blasi, F. & Dano, K. (1991). *J. Biol. Chem.* **266**, 1926–1933.
Preissner, K. T., Kanse, S. M., Chavakis, T. & May, A. E. (1999). *Basic Res. Cardiol.* **94**, 315–321.
Quax, P. H., Grimbergen, J. M., Lansink, M., Bakker, A. H., Blatter, M. C., Belin, D., van Hinsbergh, V. W. & Verheijen, J. H. (1998). *Arterioscler. Thromb. Vasc. Biol.* **18**, 693–701.
Roldan, A. L., Cubellis, M. V., Masucci, M. T., Behrendt, N., Lund, L. R., Dano, K., Appella, E. & Blasi, F. (1990). *EMBO J.* **9**, 467–474.
Ronne, E., Pappot, H., Grondahl-Hansen, J., Hoyer-Hansen, G., Plesner, T., Hansen, N. E. & Dano, K. (1995). *Br. J. Haematol.* **89**, 576–581.
Sheikh, H., Yarwood, H., Ashworth, A. & Isacke, C. M. (2000). *J. Cell. Sci.* **113**, 1021–1032.
Shliom, O., Huang, M., Sachais, B., Kuo, A., Weisel, J. W., Nagaswami, C., Nassar, T., Bdeir, K., Hiss, E., Gawlak, S., Harris, S., Mazar, A. & Higazi, A. A. (2000). *J. Biol. Chem.* **275**, 24304–24312.
Sidenius, N., Andolfo, A., Fesce, R. & Blasi, F. (2002). *J. Biol. Chem.* **277**, 27982–27990.
Sitrin, R. G., Todd, R. F. III, Mizukami, I. F., Gross, T. J., Shollenberger, S. B. & Gyetko, M. R. (1994). *Blood*, **84**, 1268–1275.
Stephens, R. W., Pollanen, J., Tapiovaara, H., Leung, K. C., Sim, P. S., Salonen, E. M., Ronne, E., Behrendt, N., Dano, K. & Vaheri, A. (1989). *J. Cell. Biol.* **108**, 1987–1995.
Stoppelli, M. P., Corti, A., Soffientini, A., Cassani, G., Blasi, F. & Assoian, R. K. (1985). *Proc. Natl Acad. Sci. USA*, **82**, 4939–4943.
Tarui, T., Mazar, A., Cines, D. B. & Takada, Y. (2001). *J. Biol. Chem.* **276**, 3983–3990.
Vassalli, J. D., Baccino, D. & Belin, D. (1985). *J. Cell Biol.* **100**, 86–92.
Vassalli, J. D., Sappino, A. P. & Belin, D. (1991). *J. Clin. Invest.* **88**, 1067–1072.
Wei, Y., Lukashev, M., Simon, D. I., Bodary, S. C., Rosenberg, S., Doyle, M. V. & Chapman, H. A. (1996). *Science*, **273**, 1551–1555.
Wei, Y., Waltz, D. A., Rao, N., Drummond, R. J., Rosenberg, S. & Chapman, H. A. (1994). *J. Biol. Chem.* **269**, 32380–32388.